Calculation of Alcohol-Acetone-Cellulose Acetate Ternary Phase Diagram and Their Relevance to Membrane Formation

JI HUA HAO, SHICHANG WANG

School of Chemical Engineering, Tianjin University, Tianjin 300072, People's Republic of China

Received 13 September 1999; accepted 20 March 2000

ABSTRACT Alcohol-acetone-cellulose acetate phase diagrams incorporated with methanol, ethanol, and isopropanol as nonsolvents are calculated according to a new form of the Flory–Huggins equation. Nonsolvent–cellulose acetate interaction parameters are measured by swelling experiments. Concentration-dependent nonsolvent–solvent interaction parameters are obtained by vapor–liquid equilibrium and the Wilson equation. It is shown that alcohol is a week coagulant compared with water, and water > methanol > ethanol > isopropanol for cellulose acetate. The phase diagrams characteristic of acetone-cellulose acetate combined with water, methanol, ethanol, and isopropanol as nonsolvents is different, which leads to the different morphological structure of a cellulose acetate membrane. The structure of a water coagulated membrane has large macrovoids from liquid–liquid phase separation. A methanol coagulated membrane has a honeycomb-like structure from spinodal microphase separation. An ethanol or isopropanol coagulated membrane has a thicker, dense top layer from the delay time phase separation. © 2001 John Wiley & Sons, Inc. J Appl Polym Sci 80: 1650–1657, 2001

Key words: phase diagram; alcohol; cellulose acetate; membrane

INTRODUCTION

The quenching step is one of the most important during the formation process of membranes made by wet and dry/wet phase inversion. In this process a homogeneous solution containing the membrane-forming polymer and a solvent for the polymer is cast as a thin film on a support or spun as a hollow fiber and contacted with a nonsolvent for the polymer. The membrane is formed[1] by an exchange of solvent and nonsolvent.

Most previous experimental studies on the formation of wet phase inversion membranes focused on water-miscible casting formulation.[2,3] But a few studies were carried out to investigate the influence of different organic quench media on the morphologies of membranes. It is evident that the choice of the quench medium can show similarly dramatic effects on the resulting structures of membranes that have the special structure and good separation performances.[4,5] However, these studies only qualitatively elucidate the influence of the quench medium on the membrane structures and lack quantitative analysis.[6] The thermodynamic diagram can be used to systematically evaluate the characteristics during the membrane-forming process. The phase diagram of water as a nonsolvent was calculated.[7,8]

Correspondence to: J. H. Hao.

Contract grant sponsor: Ph.D. Research Foundation, National Education Ministry of China.

Journal of Applied Polymer Science, Vol. 80, 1650–1657 (2001)

In this article, alcohol-acetone-cellulose acetate phase diagrams incorporated with methanol, ethanol, and isopropanol as nonsolvents were calculated according to a new form of Flory–Huggins equation.[9,10] Nonsolvent–cellulose acetate interaction parameters were measured by swelling experiments. Concentration-dependent nonsolvent interaction parameters were obtained by the methods of vapor–liquid equilibrium and the Wilson equation. Consideration was given to the behavior of the spinodal and binodal curves and tie line slopes as a function of parameters, most especially those related to the concentration dependency of the interaction parameters. The adequacy of different functional forms for the interaction parameter concentration dependence was also analyzed.

EXPERIMENTAL

Development of Equations

We used the Flory–Huggins theory for a polymer solution extended to systems with three components that was improved by Pouchly et al.[11] The Gibbs free energy of mixing (ΔG_M) is given by the following relation:

$$\Delta G_M/RT = n_1 \ln \varphi_1 + n_2 \ln \varphi_2 + n_3 \ln \varphi_3 + g_{12(u_2)} n_1 \varphi_2 + g_{13(Y_3)} n_1 \varphi_3 + g_{23(W_3)} n_2 \varphi_3 + x_{T(\varphi_1,\varphi_3)} n_1 \varphi_2 \varphi_3 \quad (1)$$

Subscripts 1–3 refer to nonsolvent, solvent, and polymer, respectively; n_i and φ_i are the number of moles and the volume fraction of component i, respectively; and R and T are the gas constant and temperature, respectively. The quantities u_1 and u_2 are given by $u_1 = \varphi_1/(\varphi_1 + \varphi_2)$, $u_2 = \varphi_2/(\varphi_1 + \varphi_2)$. The quantities Y_1 and Y_3 are given by $Y_1 = \varphi_1/(\varphi_1 + \varphi_3)$ and $Y_3 = \varphi_3/(\varphi_1 + \varphi_3)$. The quantities W_2 and W_3 are given by $W_2 = \varphi_2/(\varphi_2 + \varphi_3)$ and $W_3 = \varphi_3/(\varphi_2 + \varphi_3)$. The solvent–nonsolvent interaction parameter (g_{12}) is assumed to be a function of u_2.[9–11] The nonsolvent–polymer interaction parameter (g_{13}) is assumed to be a function of Y_3.[9,10] The solvent–polymer interaction parameter (g_{23}) is assumed to be a function of W_2.[9,10] The suggested ternary correction term was omitted because it introduces an excessive number of parameters and there are no data available for the correction term for membrane-forming systems.[8–11] Use of the definition for the chemical potential of component i relative to the pure state

$$\frac{\Delta \mu_i}{RT} = \frac{\partial}{\partial n_i} (\Delta G_M/RT)_{T,P,n_j j \neq i} \quad (2)$$

leads to the following expressions:

$$\Delta \mu_1/RT = \ln \varphi_1 + 1 - \varphi_1 - \frac{v_1}{v_2}\varphi_2 - \frac{v_1}{v_3}\varphi_3 + (g_{12}\varphi_2 + g_{13}\varphi_3)(\varphi_2 + \varphi_3) - g_{23}\frac{v_1}{v_2}\varphi_2\varphi_3 - u_1 u_2 \varphi_2 \left(\frac{dg_{12}}{du_2}\right) - \varphi_1 Y_3^2 \left(\frac{dg_{13}}{dY_3}\right) \quad (3)$$

$$\Delta \mu_2/RT = \ln \varphi_2 + 1 - \varphi_2 - \frac{v_2}{v_1}\varphi_1 - \frac{v_2}{v_3}\varphi_3 + \left(g_{12}\frac{v_2}{v_1}\varphi_1 + g_{23}\varphi_3\right)(\varphi_1 + \varphi_3) - g_{13}\frac{v_2}{v_1}\varphi_1\varphi_3 + u_1 u_2 \frac{v_2}{v_1}\varphi_1 \left(\frac{dg_{12}}{du_2}\right) - \varphi_2 w_3^2 \left(\frac{dg_{23}}{dw_3}\right) \quad (4)$$

$$\Delta \mu_3/RT = \ln \varphi_3 + 1 - \varphi_3 - \frac{v_3}{v_1}\varphi_1 - \frac{v_3}{v_2}\varphi_2 + \left(g_{13}\frac{v_3}{v_1}\varphi_1 + g_{23}\frac{v_3}{v_2}\varphi_2\right)(\varphi_1 + \varphi_2) - g_{12}\frac{v_3}{v_1}\varphi_1\varphi_2 + \varphi_3 \left[\frac{v_3}{v_1} Y_1^2 \left(\frac{dg_{13}}{dY_3}\right) + \frac{v_3}{v_2} w_2^2 \left(\frac{dg_{23}}{dw_3}\right)\right] \quad (5)$$

In eqs. (3)–(5) v_i represents the pure molar volume of species i. The solution for the binodal curve requires

$$\Delta \mu_{i,A} = \Delta \mu_{i,B}, \quad i = 1, 2, 3 \quad (6)$$

$$\sum \varphi_{i,A} = \sum \varphi_{i,B} = 1 \quad (7)$$

Subscripts A and B refer to the polymer-rich and dilute phases, respectively. Selection of one of the compositions as an independent variable leaves five coupled nonlinear algebraic equations to be solved for the individual tie lines.

The spinodal can be evaluated from the relation for ternary systems[12]:

$$G_{22} \cdot G_{33} = (G_{23})^2 \quad (8)$$

Table I Interaction Parameters of Alcohol-Cellulose Acetate

	Temperature (°C)	Density (g/cm^3)	Weight of Dry Membrane (g)	Equilibrium Absorption (g)	v_p	g_{13}
Methanol	25	0.78655	0.3256	0.0542	0.7807	1.21
Ethanol	25	0.78497	0.3042	0.0587	0.7551	1.14
Isopropanol	25	0.78091	0.3200	0.0661	0.7413	1.11

where $G_{ij} = (\partial^2 \Delta G_M / \partial \varphi_i \cdot \partial \varphi_j) v_{\text{ref}}$ and v_{ref} is the molar volume of the reference component, which in our case we take to be component 1.

From the relationship for ΔG_M (on a unit-volume basis), one has

$$(\partial \Delta G_M / \partial \varphi_2)_{T,P,\varphi_3} = \Delta\mu_2/v_2 - \Delta\mu_1/v_1 \quad (9)$$

$$(\partial \Delta G_M / \partial \varphi_3)_{T,P,\varphi_2} = \Delta\mu_3/v_3 - \Delta\mu_1/v_1 \quad (10)$$

Thus, from eqs. (3)–(5) and combined with the last two equations we can derive the necessary expressions for the spinodal.

$$G_{22} = \frac{1}{\varphi_1} + \frac{v_1}{v_2\varphi_2} - 2g_{12} + 2(u_1 - u_2)\left(\frac{dg_{12}}{du_2}\right) + u_1u_2\left(\frac{d^2g_{12}}{du_2^2}\right) - 2Y_3^3\left(\frac{dg_{13}}{dY_3}\right) + Y_1^3Y_3\left(\frac{d^2g_{13}}{dY_3^2}\right) + \frac{2v_1}{v_2}w_2^3\left(\frac{dg_{23}}{dw_3}\right) + \frac{v_1}{v_2}w_2w_3^3\left(\frac{d^2g_{23}}{dw_3^2}\right) \quad (11)$$

$$G_{23} = \frac{1}{\varphi_1} - (g_{12} + g_{13}) + \frac{v_1}{v_2}g_{23} + u_2(u_1 - 2u_2) \times \left(\frac{dg_{12}}{du_2}\right) + u_1u_2^2\left(\frac{d^2g_{12}}{du_2^2}\right) + Y_3(Y_1 - 2Y_3) \times \left(\frac{dg_{13}}{dY_3}\right) + Y_1Y_3^2\left(\frac{d^2g_{13}}{dY_3^2}\right) - \frac{v_1}{v_2}w_2^2w_3^2\left(\frac{d^2g_{23}}{dw_3^2}\right) + \frac{v_1}{v_2}w_2w_3(w_3 - w_2)\left(\frac{dg_{23}}{dw_3}\right) \quad (12)$$

$$G_{33} = \frac{1}{\varphi_1} + \frac{v_1}{v_3}\frac{1}{\varphi_3} - 2g_{13} - 2u_2^3\left(\frac{dg_{12}}{du_2}\right) + u_1u_2^3\left(\frac{d^2g_{12}}{du_2^2}\right) + 2(Y_1 - Y_3)\left(\frac{dg_{13}}{dY_3}\right) + Y_1Y_3\left(\frac{d^2g_{13}}{dY_3^2}\right) + \frac{2v_1}{v_2}w_2^3\left(\frac{dg_{23}}{dw_3}\right) + \frac{v_1}{v_2}w_3w_2^3\left(\frac{d^2g_{23}}{dw_3^2}\right) \quad (13)$$

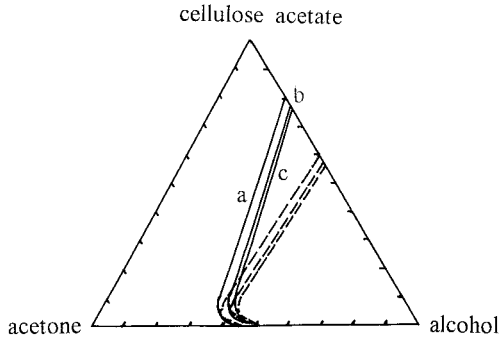

Figure 1 Phase diagrams of alcohol-acetone-cellulose acetate system for various interaction parameters (g_{13}) for (—) binodal or (–) spinodal curves: $g_{13} = 1.21$ (curve a), $g_{13} = 1.14$ (curve b), and $g_{13} = 1.1$ (curve c). Other parameters: $v_1 = 58.69$, $v_2 = 74.05$, $v_3 = 20{,}000$, $g_{12} = 0.76$, and $g_{23} = 0.2$.

To calculate the spinodal curve, one of the compositions is chosen as the independent variable that, in conjunction with the material balance ($\Sigma \varphi_i = 1$), results in a single nonlinear equation to be solved.

Method of Computation

The equation for calculating the spinodal line only deals with three variables, but the equation for calculating the binodal line deals with six variables. It is obvious that the calculation for the spinodal curve is easier than that for the binodal because the solution for the binodal can easily lead to the wrong choice and the numerical calculation of the binodals is seriously complicated. To deal with these problems, Yilmaz and McHuge[8] assumed that for large portions of the binodals, polymer compositions in the dilute phase are near zero. But their solution for the binodal has an extreme dependence on the initial guesses for the phase compositions, which must be close to the correct values. Obviously, this is difficult to achieve for all tie lines. Thus, it is still very complicated to get the binodal curves.

In order to improve the complication in the numerical calculation of the binodal, we used numerical methods for calculating phase diagrams and calculating the order that were different from the literature.[8] First we calculate the spinodal curves from eqs. (14) and (15):

Table II Concentration-Dependent Alcohol-Acetone Interaction Parameters

	$g_{12} = a + b\varphi_2$			$g_{12} = a + b\varphi_2 + c\varphi_2^2$				$g_{12} = a + b/(1 - c\varphi_2)$				$g_{12} = a + b\varphi_2 + c\varphi_2^2 + d\varphi_2^3 + e\varphi_2^4$					
System	a	b	Sum of Squares	a	b	c	Sum of Squares	a	b	c	Sum of Squares	a	b	c	d	e	Sum of Squares
H_2O-acetone [8]				1.141	0.457	1.528	1.78×10^{-2}	0.661	0.417	0.755	1.5×10^{-4}						
Methanol-acetone																	
g_{12v}	0.4558	0.4125	6.22×10^{-3}	0.5395	0.04147	0.3290	3.29×10^{-3}	0.1210	0.3918	0.5086	3.39×10^{-3}						
g_{12w}	0.5441	0.4381	4.72×10^{-3}	0.6019	0.1018	0.3272	1.44×10^{-4}	0.1772	0.4116	0.5211	9.0×10^{-6}						
Ethanol-acetone																	
g_{12v}	0.3754	0.01213	5.66×10^{-2}	0.4477	−0.3619	0.3709	5.50×10^{-2}	0.3723	0.007006	1.5113	3.21×10^{-2}	0.5882	−1.0301	−2.4304	11.4891	−8.7928	6.5×10^{-3}
g_{12w}	0.6668	0.1706	2.85×10^{-4}	0.6834	0.0840	0.08255	9.46×10^{-5}	0.4182	0.2631	0.3951	1.16×10^{-6}						
Isopropanol-acetone																	
g_{12v}	1.2926	−0.5667	0.12	1.0464	0.9048	−1.6892	7.74×10^{-2}	1.0324	−0.03065	6.687	8.36×10^{-2}						
g_{12w}	1.1816	−0.7463	9.24×10^{-3}	1.2901	−1.3945	0.7441	3.14×10^{-4}	0.1359	1.2151	−1.7519	9.73×10^{-6}						

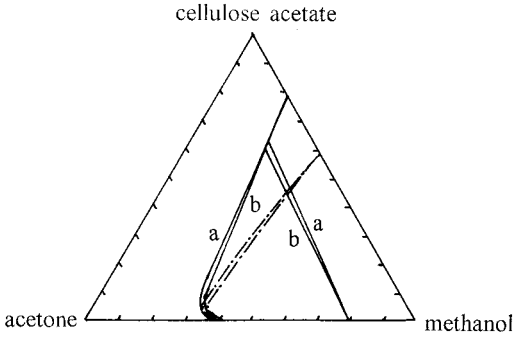

Figure 2 Phase diagrams for methanol-acetone-cellulose acetate system for (—) binodal curves and (– · –) spinodal curves: $g_{12v} = 0.5395 + 0.04147u_2 + 0.3290u_2^2$ (curve a) and $g_{12w} = 0.6019 + 0.1018u_2 + 0.3272u_2^2$ (curve b). Other parameters: $v_1 = 40.73$, $v_2 = 74.05$, $v_3 = 20{,}000$, $g_{13} = 1.21$, and $g_{23} = 0.2$.

$$f_1 = G_{22}G_{33} - (G_{23})^2 \tag{14}$$

$$f_2 = \varphi_1 + \varphi_2 + \varphi_3 - 1 \tag{15}$$

The φ_3 was selected as the independent variable, and $F(\varphi) = \Sigma f_i^2$ was used as the objective function.

The mixed computation of the Newton–gradient was used to solve the nonlinear equations, which kept the characteristics of the gradient stability and the Newton fast convergence. We applied the imitation Newton method to replace the Jacobean matrix and its reverse skill. We show that the spinodal compositions did not rely completely on whether the initial guesses were close to the correct values, and its solution vector was

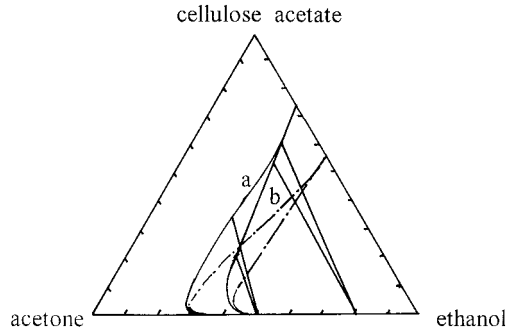

Figure 3 Phase diagrams for ethanol-acetone-cellulose acetate system for (—) binodal curves, (– · –) spinodal curves, and tie lines: $g_{12v} = 0.5882 - 1.0301u_2 - 2.4394u_2^2 + 11.4891u_2^3 - 8.7928u_2^4$ (curve a) and $g_{12w} = 0.6834 + 0.0840u_2 + 0.08255u_2^2$ (curve b). Other parameters: $v_1 = 58.69$, $v_2 = 74.05$, $v_3 = 20{,}000$, $g_{13} = 1.14$, and $g_{23} = 0.2$.

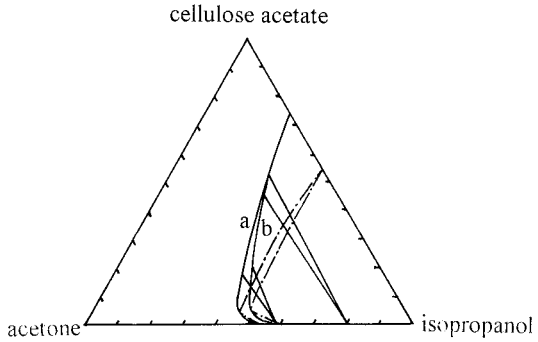

Figure 4 Phase diagrams for isopropanol-acetone-cellulose acetate system for (—) binodal curves, (– · –) spinodal curves and tie lines: $g_{12v} = 1.0464 + 0.9048u_2 - 1.6892u_2^2$ (curve a) and $g_{12w} = 1.2901 - 1.3945u_2 + 0.7441u_2^2$ (curve b). Other parameters: $v_1 = 76.05$, $v_2 = 74.05$, $v_3 = 20{,}000$, $g_{13} = 1.11$, and $g_{23} = 0.2$.

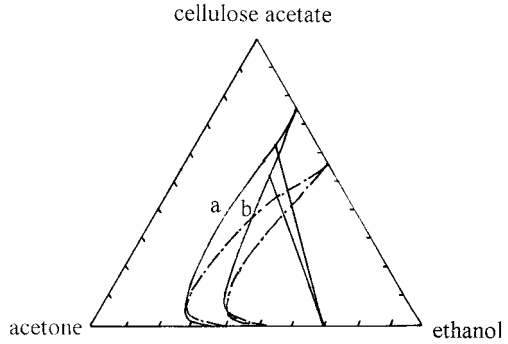

Figure 6 Phase diagrams for ethanol-acetone-cellulose acetate system for (—) binodal curves, (– · –) spinodal curves, and tie lines: $g_{12v} = 0.5882 - 1.0301u_2 - 2.4394u_2^2 + 11.4891u_2^3 - 8.7928u_2^4$ (curve a) and $g_{12w} = 0.6668 - 0.1706u_2$ (curve b). Other parameters: $v_1 = 58.69$, $v_2 = 74.05$, $v_3 = 20{,}000$, $g_{13} = 1.14$, and $g_{23} = 0.535 + 0.11W_3$.

stable. Because the spinodal and binodal curves coincide at a critical point, the reliability of the spinodal curves assured the correctness of the binodal curve. Therefore, we can be sure to choose which solution is correct. The computation of the binodal curve gets easier in combination with Yilmaz and McHuge's experience.[8]

RESULTS AND DISCUSSION

Measurement of Alcohol-Cellulose-Acetate Interaction Parameter and Its Effect on Phase Diagram

Cellulose acetate dense membranes were prepared according to the literature.[13] Their density was 1.327 g/cm^3. The interaction parameter (g_{13}) can be measured by the swelling equilibrium method[14] and can be calculated as follows:

$$g_{13} = -[\ln(1 - v_p) + v_p]/v_p^2 \qquad (16)$$

As shown in Table I, the g_{13} of alcohol-cellulose acetate was in order of methanol, ethanol, isopropanol ($g_{13\text{methanol}} > g_{13\text{ethanol}} > g_{13\text{isopropanol}}$), which illustrates that the affinity between alcohol and cellulose acetate increases in order (methanol < ethanol < isopropanol). Compared with water ($g_{13\text{water}} = 1.4$), precipitation of cellulose acetate solution becomes weak and gets slower in the water, methanol, ethanol, and isopropanol order.

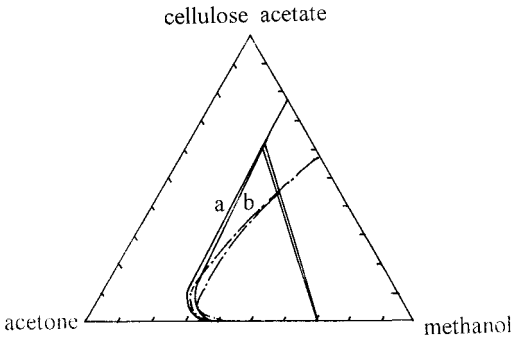

Figure 5 Phase diagrams for methanol-acetone-cellulose acetate system for (—) binodal curves, (– · –) spinodal curves, and tie lines: $g_{12v} = 0.121 + 0.3918/(1 - 0.5086u_2)$ (curve a) and $g_{12w} = 0.1772 + 0.4116/(1 - 0.5271u_2)$ (curve b). Other parameters: $v_1 = 40.73$, $v_2 = 74.05$, $v_3 = 20{,}000$, $g_{13} = 1.21$, and $g_{23} = 0.535 + 0.11W_3$.

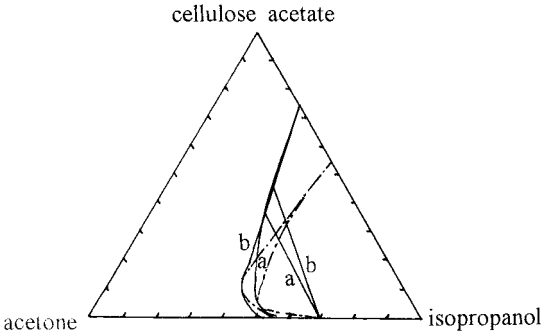

Figure 7 Phase diagrams for isopropanol-acetone-cellulose acetate system for (—) binodal curves, (– · –) spinodal curves, and tie lines: $g_{12v} = 1.0464 + 0.9048u_2 - 1.6892u_2^2$ (curve a) and $g_{12w} = 1.2901 - 1.3945u_2 + 0.7441u_2^2$ (curve b). Other parameters: $v_1 = 76.92$, $v_2 = 74.05$, $v_3 = 20{,}000$, $g_{13} = 1.11$, and $g_{23} = 0.535 + 0.11W_3$.

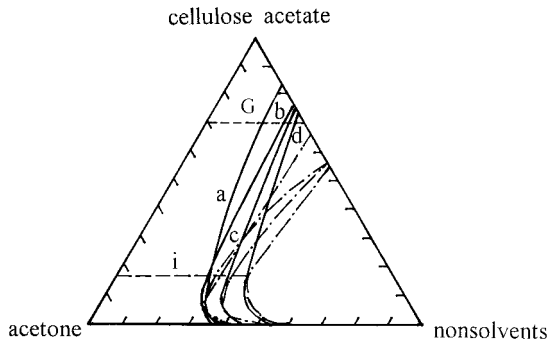

Figure 8 Phase diagrams of nonsolvent-acetone-cellulose acetate system. Curves a–d represent the respective coagulants: water, methanol, ethanol, and isopropanol for (—) binodal curves, (– · –) spinodal curves, (——) the cellulose acetate concentration of the initial casting solution (i), and (—) the glass transition (G).

The miscibility gap on the phase diagrams correspondingly increased as shown in Figure 1.

Calculation of Acetone-Alcohol Interaction Parameter and Its Effect on Phase Diagram

From eq. (1), when $\varphi_3 = 0$, Flory–Huggins theory can be simplified to solvent–nonsolvent systems; the following expression would result:

$$g_{12} = [\Delta G_M/RT - \chi_1 \ln \varphi_1 - \chi_2 \ln \varphi_2]/\chi_1\varphi_2 \quad (17)$$

From the relation between the excess Gibbs energy (G^E) and the Gibbs free energy of mixing for a two-component system, the parameters can be calculated from literature data on G^E.[15–17]

$$g_{12} = [\chi_1 \ln(\chi_1/\varphi_1) + \chi_2 \ln(\chi_2/\varphi_2) + G^E/RT]/\chi_1\varphi_2 \quad (18)$$

As shown in Table II, the g_{12} of acetone with methanol, ethanol, and isopropanol was calculated from the G^E, which was obtained from a vapor pressure experiment, and was related by the Wilson equation.[18] Table II shows the range of coefficients found for typical system fits and also gives an indication of the suitability of a given correlation form. In all cases the coefficients were determined via a modified Marquardt nonlinear regression algorithm.[19]

The inclusion of different concentration-dependent forms produced significant changes in the phase diagram. Figures 2–4 illustrate several characteristics in the behavior of the binodal and spinodal curves resulting from use of different concentration-dependent g_{12} values, which have the qualitative features as well, such as shapes, miscibility gap, slopes of the tie lines, and so forth. In such a fashion, one can gain an appreciation of the effect of the concentration dependence on the membrane formation processes and membrane structure.

Calculation of Thermodynamic Phase Diagrams for Alcohol-Acetone-Cellulose Acetate Systems

As pointed out earlier, the principal reason for employing concentration-dependent forms for the interaction parameters was to improve the accuracy of the phase diagrams predicted from Flory–Huggins theory. In order to obtain the more accurate phase diagrams for alcohol-acetone-cellulose acetate systems, we simultaneously calculated the phase diagrams with the concentration-dependent forms of g_{12} and g_{23} shown in Figures 5–7.

Figures 5–7 illustrate typical effects on the phase diagrams resulting from use of the W_3 concentration-dependent g_{23} as compared to constant values. For the cases of methanol and ethanol as nonsolvents, the binodal curves and spinodal curves were closer to the cellulose acetate–acetone axis. But for isopropanol the result was the opposite. The miscibility gap became wider. These results showed the critical role of the concentration dependence of the solvent–polymer interaction parameter in affecting the nature of the predicted miscibility.

Thermodynamic Analysis of Membrane-Forming Systems

For comparison, the phase diagram of water as a coagulant is shown in Figure 8. Generally, the single phase region between the binodal and cellulose acetate-acetone axis increases gradually in the order of water, methanol, ethanol, and isopropanol; thus, the cast solution becomes more stable. A microphase separation process may be more difficult. According to work by Reuvers and Smolders,[20] the casting membrane of cellulose acetate-acetone solution into water during membrane formation may reach phase separation after a certain time interval. We deduced that a similar phase separation may happen to other coagulants (methanol, ethanol, isopropanol), and in that order the delay time may be gradually prolonged. The thickness of the concentrated

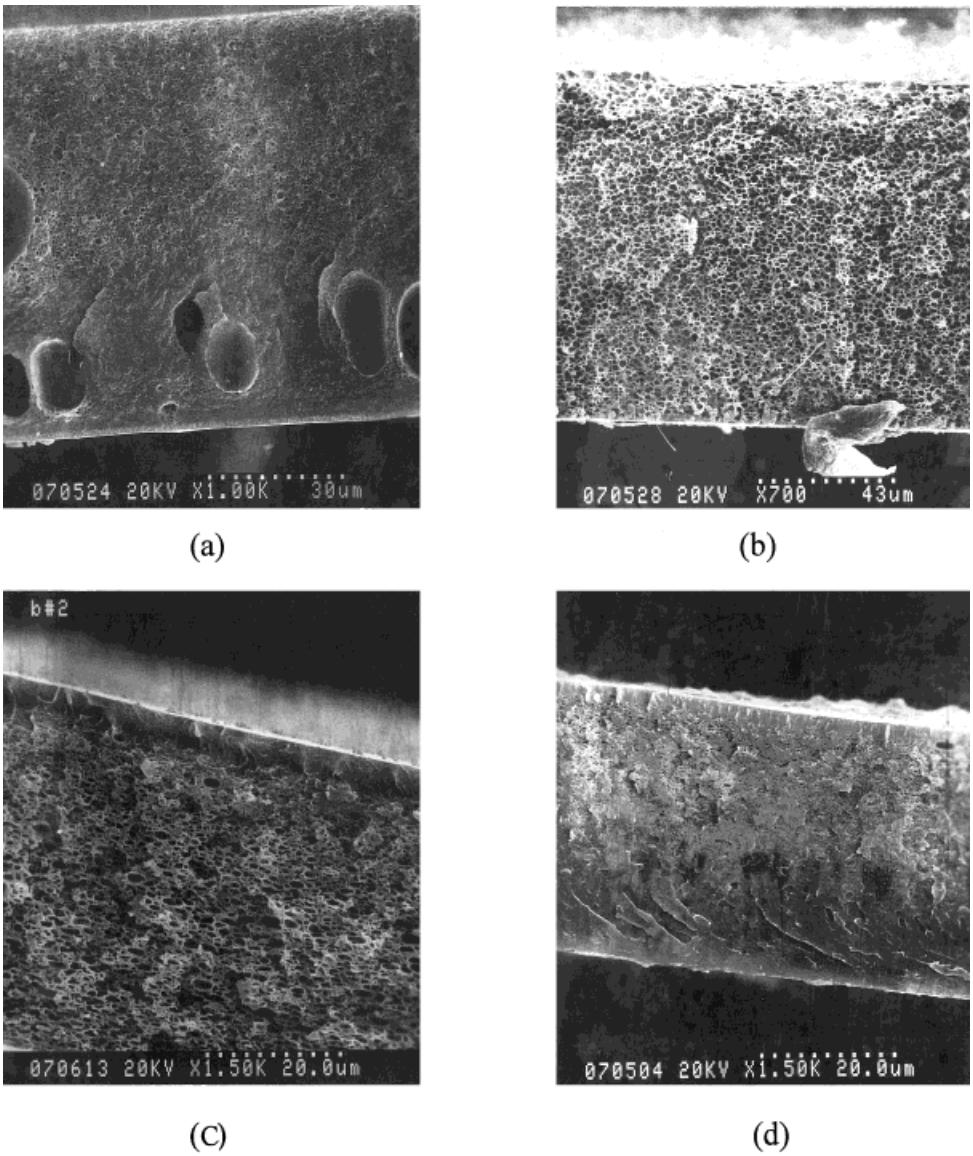

Figure 9 The structure of a cellulose acetate membrane in different quenches made by wet phase inversion without evaporation: (a) water, (b) methanol, (c) ethanol, and (d) isopropanol.

layer in the top section increased with the square root of the delay time. As shown in Figure 9, the skin thickness and transition region become thicker in the order of a methanol, ethanol, or isopropanol quenched membrane. During the delay time, the top surface of the ethanol or isopropanol quenched membrane are concentrated enough to avoid the form of the defect-free skin layer on the set of the phase separation. When the cast cellulose acetate concentration is low (10–20 vol %), the binodal of the methanol coagulant is nearest the cellulose acetate–acetone axis. So the methanol quenched membrane without evaporation may undergo a spinodal decomposition with nodular structures as shown in Figure 9(b), which will lead to a honeycomb-like structure. With the increase of cellulose acetate concentration the metastable regions between the binodal and spinodal boundaries are reduced. The phase separation changes smoothly from a spinodal deposition to a nucleation and growth process until the gelation transition. At that time, the binodal of the methanol coagulant deviates from that of the water coagulant and approaches that of the ethanol by degrees. Therefore, the phase separation feature of the methanol quenched membrane at the

high cellulose acetate concentration is more similar to that of the ethanol quenched membrane. This is why the top skin layer of the methanol quenched membrane with an evaporation time of 40 s is defect free.[21] But methanol must penetrate into the dense skin.[10] When the nascent membranes were immersed in water, the membranes were solidified immediately. However, because water cannot immediately diffuse into the casting solution under the top layer, water will accumulate at the local area, which leads to the formation of large fingerlike morphological structure of the membranes, as shown in Figure 4(a). We hope to report on these data and analyses in future publications.

CONCLUSION

The thermodynamic phase diagrams for alcohol-acetone-cellulose acetate systems incorporated with methanol, ethanol, and isopropanol as nonsolvents were calculated according to a new form of Flory–Huggins equation.

The choice of the quench medium is of the utmost importance for the characteristics of phase diagrams, which leads to different morphological structures. The structure of a water coagulated membrane had large macrovoids from liquid–liquid phase separation. The methanol quenched membranes without evaporation showed spinodal decomposition. The ethanol or isopropanol coagulated membrane displayed a dense and rather thick top layer supported by a closed cell spongelike substructure from the delay time phase separation.

REFERENCES

1. Tsay, C. S.; McHugh, A. J. J Polym Sci Polym Phys Ed 1990, 28, 1327.
2. Frommer, M. A.; Lancet, D. Polym Prepr 1971, 12, 245.
3. Tweedle, T. A.; Kutowy, O.; Thayer, W. L.; Sourirajan, S. Ind Eng Chem Prod Res Dev 1983, 22, 320.
4. Mulder, M. H. V.; Oude Hendrikman, J.; Wijmans, J. G.; Smolder, C. A. J Appl Polym Sci 1985, 30, 2805.
5. Pinnau, I.; Koros, W. J. J Membr Sci 1992, 71, 81.
6. Radovanovic, P.; Thiel, S. W.; Hwang, S. T. J Membr Sci 1992, 65, 213.
7. Altena, F. W.; Smolders, C. A. Macromolecules 1982, 15, 1491.
8. Yilmaz, L.; McHuge, A. J. J Appl Polym Sci 1986, 31, 997.
9. Hao, J. H.; Wang, S. C. Chem J Ch Univ 1995, 16, 1831.
10. Hao, J. H. Ph.D. Thesis, Tianjin University, Tianjin, 1995.
11. Pouchly, J.; Zivney, A.; Sole, K. J Polym Sci Polym Symp 1968, 23, 245.
12. Tompa, H. Polymer Solution; London: Butterworths, 1956; p 182.
13. Puleo, A. C.; Paul, D. R. J Membr Sci 1989, 47, 301.
14. Mulder, M. H. V.; Franken, T.; Smolders, C. A. J Membr Sci 1985, 21, 155.
15. Campbell, A. N.; Anand, S. C. Can J Chem 1972, 50, 479.
16. Kato, M. Bull Chem Soc Jpn 1982, 55, 23.
17. Puri, P. S.; Polak, J.; Ruether, J. A. J Chem Eng Data 1974, 19, 87.
18. Gemhling, J.; Onken, U.; Arlt, W. Chemical Data Series; Germany: Schon and Wetzel Gmbh, 1978; Vol. 1, Part 2C, p XXXII.
19. Liu, D. G.; Fei, J. G.; Yu, Y. J. Newly Practical Algorithm for the Engineering and the Fortran Procedure; Beijing: National Defence Industry Press, 1990; p 363.
20. Reuvers, A. J.; Smolders, C. A. J Membr Sci 1987, 34, 67.
21. Hao, J. H.; Wang, S. C. J Appl Polym Sci 1998, 68, 1269.